Tree Physiology 38, 198–211
doi:10.1093/treephys/tpx140

Research paper

Acclimation of branch and leaf hydraulics in adult *Fagus sylvatica* and *Picea abies* in a forest through-fall exclusion experiment

Martina Tomasella[1,3], Barbara Beikircher[2], Karl-Heinz Häberle[1], Benjamin Hesse[1], Christian Kallenbach[1], Rainer Matyssek[1] and Stefan Mayr[2]

[1]Department of Ecology and Ecosystem Management, Chair for Ecophysiology of Plants, Technical University of Munich, Hans-Carl-von-Carlowitz Platz 2, 85354 Freising, Germany; [2]Department of Botany, University of Innsbruck, Sternwartestraße 15, 6020 Innsbruck, Austria; [3]Corresponding author (martina.tomasella@tum.de)

Received July 11, 2017; accepted October 3, 2017; published online November 21, 2017; handling Editor Frederick Meinzer

Decreasing water availability due to climate change poses the question of whether and to what extent tree species are able to hydraulically acclimate and how hydraulic traits of stems and leaves are coordinated under drought. In a through-fall exclusion experiment, hydraulic acclimation was analyzed in a mixed forest stand of *Fagus sylvatica* L. and *Picea abies* (L.) Karst. In drought-stressed (TE, through-fall exclusion over 2 years) and control (CO) trees, hydraulic vulnerability was studied in branches as well as in leaves (*F. sylvatica*) and end-twigs (*P. abies*, entirely formed during the drought period) sampled at the same height in sun-exposed portions of the tree crown. In addition, relevant xylem anatomical traits and leaf pressure–volume relations were analyzed. The TE trees reached pre-dawn water potentials down to −1.6 MPa. In both species, water potentials at 50% loss of xylem hydraulic conductivity were ~0.4 MPa more negative in TE than in CO branches. Foliage hydraulic vulnerability (expressed as water potential at 50% loss of leaf/end-twig hydraulic conductance) and water potential at turgor loss point were also, respectively, 0.4 and 0.5 MPa lower in TE trees. Minor differences were observed in conduit mean hydraulic diameter and cell wall reinforcement. Our findings indicate significant and fast hydraulic acclimation under relatively mild drought in both tree species. Acclimation was well coordinated between branches and foliage, which might be essential for survival and productivity of mature trees under future drought periods.

Keywords: drought, leaf hydraulic conductance, plasticity, rehydration kinetics, safety margins, turgor loss, vulnerability to cavitation, xylem anatomy.

Introduction

Water limitation is one of the most critical challenges to plant survival and productivity in light of the ongoing climate change. Shifts in precipitation and temperature patterns in Europe, as in other regions of the world (Dai 2013), lead to extended and more frequent droughts during the growing season (Fuhrer et al. 2006) and to more recurrent dry years (Briffa et al. 2009). Such environmental constraints have induced, in extreme cases, episodes of tree dieback reported worldwide (e.g., Allen et al. 2010, Nardini et al. 2013). Embolism, owing to increased xylem tensions and subsequent entry of gaseous bubbles into the conduits (Tyree and Zimmermann 2002), is thought to be a main mechanism causing dieback or even death of individuals through reduction of xylem hydraulic conductivity (hydraulic failure; McDowell et al. 2008).

Plant-functional traits can be used as predictors of plant population abundance dynamics and species distribution under climate change (Soudzilovskaia et al. 2013). During changing environmental conditions, the survival of long-lived woody plants depends not only on the species' general resistance but also on their acclimation potential, i.e., the capability to adjust structural and/or functional traits to environmental changes within their life-span (Beikircher and Mayr 2009, Taiz and Zeiger 2010). A high phenotypic plasticity, which is the ability of a genotype to express different phenotypes in response to environmental

factors (Sultan 2000), may thus allow individuals to better acclimatize to changing climate conditions. Acclimation differs from adaptation, which instead implies the occurrence of genetic changes, over many generations and through natural selection (Debat and David 2001). Accordingly, species-specific predisposition to tolerate drought (Maherali et al. 2004) reflects adaptations to withstand mean stress levels, while a plastic response in cavitation resistance may play a central role for trees undergoing repeated drought events. It would allow trees to sustain more negative water potentials without incurring hydraulic failure during consecutive droughts.

Despite its importance, however, the degree of phenotypic plasticity in hydraulic traits under drought is still poorly understood (Anderegg 2015). For example, cavitation resistance has been claimed to be a plastic feature in some species (Jacobsen et al. 2007, Beikircher and Mayr 2009), but not in others (Martinez-Vilalta et al. 2009, Lamy et al. 2014), and evidence on hydraulic acclimation in leaves is largely absent (Martorell et al. 2015).

The available studies on tree hydraulic acclimation are based either on spatial or temporal analyses. The first category mainly includes population comparisons along precipitation gradients (e.g., Cornwell et al. 2007, Schuldt et al. 2016), in which site effects have to be considered (Goldstein et al. 2013, Tokumoto et al. 2014). The second category comprises greenhouse/garden experiments performed mainly on juvenile trees (e.g., Aranda et al. 2015, Martorell et al. 2015) or dendrochronological analyses on mature trees (e.g., Montwé et al. 2014, Rita et al. 2015). A third type of temporal acclimation analysis is based on precipitation exclusion experiments, which, inducing drought stress on a small scale, allow for direct measurements of species' hydraulic adjustment potentials. Nevertheless, especially for hydraulic studies on trees, this approach has rarely been used (Martin-StPaul et al. 2013, Montwé et al. 2014).

The hydraulic vulnerability segmentation hypothesis (Tyree and Ewers 1991) predicts that distal segments of a tree have lower resistance to cavitation than the proximal segments to which they are connected. This would be beneficial for trees undergoing drought because distal components cavitate first, causing the reduction of tensions in the central and more 'expensive' segments and limiting further water losses by disconnecting leaves from the hydraulic system. The hydraulic segmentation of a branch can be characterized by its leaf-to-stem safety margin (for other definitions of safety margins see, e.g., Johnson et al. 2012*a*), expressed as the difference between the water potential inducing 50% loss of leaf conductance (Ψ_{50_leaf}) and the water potential inducing 50% loss of branch xylem conductance (Ψ_{50_branch}). So far, only a few studies have directly compared stem and leaf vulnerabilities (Johnson et al. 2011, 2016, Beikircher et al. 2013, Scholz et al. 2014, Nolf et al. 2015) and no analysis on drought acclimation and respective changes of leaf-to-stem hydraulic safety margins is available. Furthermore, the coordination with other hydraulic leaf traits is not well understood. In leaves, osmotic adjustment is the main driver for maintaining turgor at more negative water potentials (Bartlett et al. 2012) and has been suggested to contribute to the acclimation of leaf hydraulic vulnerability under drought (Martorell et al. 2015).

In the present study, we investigated the acclimation potentials of the angiosperm European beech (*Fagus sylvatica* L.) and the coniferous Norway spruce (*Picea abies* (L.) Karst), which dominate managed forests in Central Europe, covering 30% of the forested area (Pretzsch et al. 2014). Hydraulic studies on adult trees of these important species are scarce and focused on within-tree and population comparisons (Herbette et al. 2010, Schuldt et al. 2016). In *P. abies* only a study on wood anatomical plasticity is available (Montwé et al. 2014) and in *F. sylvatica* hydraulic acclimation to changing light conditons was observed in branches (Lemoine et al. 2002, Herbette et al. 2010) and to drought in potted saplings (Aranda et al. 2015). These species are also interesting from a hydraulic point of view, as *F. sylvatica* is known to follow an overall more anisohydric and *P. abies* a more isohydric strategy (Lyr et al. 1992). A through-fall exclusion experiment enabled us to study mature trees within a mixed forest and thus to simulate drought in an otherwise intact forest system. After 2 years of through-fall exclusion, we examined (i) the acclimation in the vulnerability to xylem cavitation at the branch level, (ii) changes in xylem anatomical traits related to cavitation resistance, (iii) the acclimation in the vulnerability of leaves (*F. sylvatica*) and end-twigs (*P. abies*) and (iv) adjustments of the leaf turgor loss point. We expected stronger hydraulic acclimation in *F. sylvatica*, as safety margins in angiosperms are usually small (enabling only limited protection under prolonged drought) and wood formation, due to the presence of several different cell types, is probably plastic. In contrast, in *P. abies*, we hypothesized smaller plastic responses. This would be in accordance with a recent meta-analysis (Anderegg 2015), in which angiosperms showed higher intraspecific variability in hydraulic traits than conifers.

Materials and methods

Experimental site and plant material

The study site is located in the Kranzberg Forest, Southern Bavaria, Germany (N48°25′12″, W11°39′42″, elevation 450 m above sea level). Mean annual air temperature is 7.8 °C and mean precipitation 750–800 mm year^{-1}, whereas during the growing seasons (May–September) the respective values are 13.8 °C and 460–500 mm year^{-1} (averaged from 1971 to 2000, Hera et al. 2011). The site is characterized by a mixed stand of European beech (*F. sylvatica*) and Norway spruce (*P. abies*) with a mean age of 83 ± 4 years and 63 ± 2 years, respectively (2014). The trees belong to study plots included in the 'Kranzberg ROOF experiment' (KROOF, Goisser et al. 2016, Pretzsch et al. 2016). Each plot (sizes ranging between 110 and

200 m^2) included four to six *F. sylvatica* and a similar number of *P. abies* specimens. The plots were trenched in spring 2010 by vertical ditches down to 1 m soil depth (reaching a dense clay layer of tertiary sediments), subsequently lined with plastic tarp (waterproof and impermeable to root growth), and refilled with soil. Since May 2014, rainfall has been excluded at 6 out of 12 plots by means of automated roofs at ~3 m aboveground, which from April–May to November were closed in case of precipitation (Pretzsch et al. 2016). During winter, the roofs were permanently open.

The plant material was sampled in eight plots (four unroofed, control (CO); four roofed, with TE), in which tree crowns were accessible through a canopy crane. Branches and single leaves (*F. sylvatica*) or end-twigs (*P. abies*) were taken from sun-exposed crown parts at ~30 m height, corresponding to the upper canopy of *F. sylvatica* trees. The sampling was strictly performed at this height to avoid shading (Lemoine et al. 2002) or height (Ambrose et al. 2009) effects on the studied hydraulic parameters. We used end-twigs for analyses in case of *P. abies* because the small needles of this species allow neither pressure–volume analyses nor rehydration kinetics measurements (see 'Materials and methods' section). Still, this enabled us to characterize hydraulics of distal crown parts and should sufficiently represent needle hydraulics. It is important to note that the entire end-twigs analyzed were grown from 2014 to 2016, when the rainfall exclusion experiment was performed.

The experimental drought applied in 2015 and 2016 strongly limited growth of *P. abies* TE trees, i.e., in 2016 the current and the previous year shoots were extremely short in comparison with CO twigs (max. 2 cm length, Figure 1d and see Figure S1 available as Supplementary Data at *Tree Physiology* Online). For this reason, measurements (pressure–volume and leaf vulnerability analysis; see 'Materials and methods' section) on *P. abies* were performed on 3-year-old end-twigs (i.e., built since spring 2014). The CO and TE end-twigs used for measurements were 17.4 ± 0.7 and 12.6 ± 1.2 cm long, respectively. In order to identify potential effects of the current and previous year shoot (differently developed in CO and TE end-twigs), additional measurements were performed on 3-year-old segments, deprived of the current year and the previous year segments (abbreviation CO_{year3}). A scheme with all measurements performed is given in Figure 1.

Soil volumetric water content

Soil volumetric water content (SVWC, %) was measured weekly via time domain reflectometry (TDR 100, Campbell Scientific, Inc., Logan, UT, USA) in all experimental plots (six CO and six TE). Time domain reflectometry probes were installed in the middle of each plot at four different depths (0–7 cm, 10–30, 30–50 and 50–70 cm). In the results are reported the SVWC values measured at the shallower (0–7 cm) and deeper (50–70 cm) layers.

Pre-dawn and minimum seasonal water potentials

Pre-dawn water potentials (Ψ_{pd}) were measured in several campaigns over all growing seasons (2014–16). One short end-twig was excised from each of eight trees per treatment and species at ~30 m height, between 03:00 and 04:30 h solar time (before sunrise). Immediately after harvest, samples were sealed in plastic bags and water potential was measured, using a pressure chamber (Model 3000 Pressure Extractor, Soilmoisture Equipment Corp., Santa Barbara, CA, USA).

Midday water potentials (Ψ_{md}) were measured during several campaigns in summer 2016 (last year of drought) as described above, between 12:00 and 14:30 h (sunny days). Minimum water potentials (per species and treatment) were defined as the lowest Ψ_{md} reached during the growing season (corresponding to the July or August campaigns). These values, compared with branch xylem and leaf/end-twig vulnerabilities (see below), allowed estimation of the stomatal regulation in relation to leaf and branch hydraulic dysfunction.

Branch xylem vulnerability curves

Vulnerability to xylem cavitation was assessed with the Cavitron technique (Cochard et al. 2005) in seven to eight trees per treatment (CO and TE), taking one branch per tree. Samples were collected between February and March 2016 (2 years after starting the through-fall exclusion), i.e., when the roofs of TE plots had been kept open for the whole winter (from December 2015) and prior spring flush, to avoid influences of phenological differences between trees on vulnerability analysis. After harvest, the cut ends of *F. sylvatica* and *P. abies* branches were shortened under water. *Fagus sylvatica* samples (placed in buckets with water) and *P. abies* samples (wrapped tightly in plastic bags containing wet paper towels) were transported within 1 day to Innsbruck (Institute of Botany) for vulnerability measurements. Side twigs were removed and the main stem was re-cut several times under water according to Beikircher and Mayr (2016), until reaching a length of 27.5 cm. The mean diameter of samples (without bark) ranged between 3.5 and 5.5 mm in *F. sylvatica* and between 5.0 and 7.0 mm in *P. abies*, while the central portion of the stem segments was 2–3 years old in *F. sylvatica* and 3 years old in *P. abies*. This implies that most of TE branches used for Cavitron and xylem anatomical analysis (see below) included xylem built the year before the start of through-fall exclusion. *Fagus sylvatica* segments were debarked (5 cm) at both ends; in *P. abies*, bark was removed from the entire sample, to avoid clogging of tracheids by resin. Immediately before Cavitron (Cochard 2002) measurements, *F. sylvatica* segments were flushed at 0.08 MPa for 20 min at both cut ends (until reaching maximum conductivity), while connected to the Xylem Embolism Meter (XYL'EM, Bronkhorst, France), in order to remove native embolism. Native embolism in *F. sylvatica* was 44 ± 12% (no difference between treatments), due to winter embolism, while no native embolism was detected in *P. abies*.

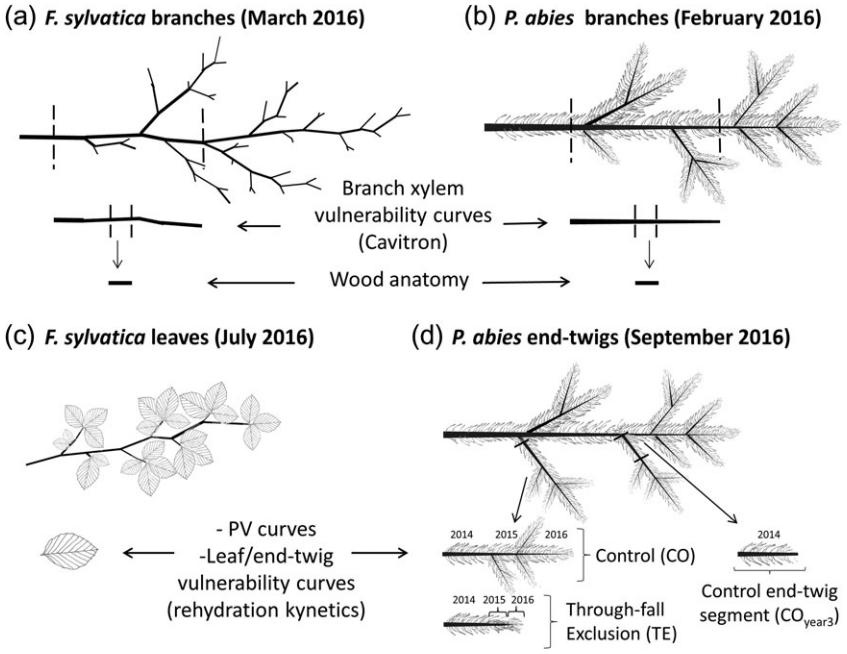

Figure 1. Scheme of measurements and plant material. Branch (a and b) xylem vulnerability analyses were performed with the Cavitron technique in February–March 2016 using the main branch. The central segment of the sample was used afterwards for anatomical analysis. Pressure–volume (PV) curves and leaf/twig vulnerability curves were performed in leaves (*Fagus sylvatica*, c) or end-twigs (*P. abies*, d) in summer 2016. Leaf/end-twig vulnerabilities were analyzed by progressively dehydrating branches and then detaching single leaves/end-twigs in the lab for rehydration kinetics procedure. For measurements, control (CO) and drought-stressed (TE) trees were used. In case of *P. abies* CO end-twigs, also samples lacking the previous and current year shoot were prepared (CO_{year3}, called 'control end-twig segments' in the text). The CO and TE end-twigs of *P.abies* were grown from 2014 to 2016, when the rainfall exclusion experiment was performed.

Cavitron measurements and conductivity calculations followed Beikircher et al. (2010). After final trimming at both ends, samples were fixed in a 280 mm custom-built rotor inside a centrifuge (Sorvall RC-5, Thermo Fisher Scientific, Waltham, MA, USA). Segment ends were kept inside transparent plastic reservoirs filled with distilled, filtered (0.22 m) and degassed water containing 0.005% (v/v) 'Micropur' (Katadyn Products Inc., Wallisellen, Switzerland) to prevent microbial growth. Hydraulic conductivity (k) through the sample was calculated at successive higher xylem pressures, induced by increasing rotational speed. Percentage loss of conductivity (PLC) was calculated as:

$$PLC = 100(1 - k_f/k_i) \quad (1)$$

where k_i is the initial (maximum) hydraulic conductivity (obtained at a xylem pressure below 0.5 MPa) and k_f is the hydraulic conductivity at the xylem water potential at a given rotational speed (Ψ_{xylem}).

Curves were fitted with the software package R (R Development Core Team 2014, version 3.1.2) using an exponential sigmoidal function, according to Pammenter and Vander Willingen (1998):

$$PLC = 100/1 + exp[a_{branch}(\Psi_{xylem} - \Psi_{50\_branch})] \quad (2)$$

where a_{branch} is the coefficient related to the slope of the curve and Ψ_{50_branch} is the branch xylem water potential inducing 50% loss of conductivity. The xylem pressures inducing 12 (Ψ_{12_branch}) and 88 (Ψ_{88_branch}) PLC were also calculated:

$$\Psi_{12\_branch} = \log(100/12 - 1)/a + \Psi_{50} \quad (3)$$

$$\Psi_{88\_branch} = \log(100/88 - 1)/a + \Psi_{50} \quad (4)$$

Wood anatomical analysis

In order to relate xylem anatomical traits to the potential hydraulic plasticity under drought, conduit mean arithmetic diameter (D, μm), conduit mean hydraulic diameter (D_h, μm), conduit wall reinforcement $(t/b)_h^2$, conduit density (CD) and vessel grouping index (V_G, only for *F. sylvatica*) were calculated from xylem cross section analysis.

From the central portion of five randomly selected samples per treatment previously used for vulnerability curves, cross sections of 15–20 μm thickness were obtained with a microtome (Sledge Microtome G.S.L. 1, Schenkung Dapples, Zürich, Switzerland) and stained with Etzold FCA mixture. Anatomical traits were analyzed from pictures captured with a digital camera (ProgRes CT3, Jenoptik, Jena, Germany) connected to a light microscope (Olympus BX41TF, Olympus Austria, Vienna, Austria), at a magnification of 20× for *F. sylvatica* and 40× for *P. abies*. For each section, analyses were conducted on a radial sector of sapwood including all relevant annual rings (3 years, formed from 2013 to 2015). Images were analyzed using the

software ImageJ (v. 1.48; US National Institutes of Health, Bethesda, MD, USA, http://imagej.nih.gov/ij/).

D_h was calculated according to the equation (Sperry and Hacke 2004):

$$D_h = \frac{\sum D^5}{\sum D^4} \quad (5)$$

where D is the conduit diameter, calculated from the conduit area and assuming a circular shape in *F. sylvatica* and a squared shape in *P. abies*.

Conduit wall reinforcement $(t/b)_h^2$ was calculated according to Hacke et al. (2001*a*), whereby t is the thickness of the double cell wall and b the hydraulic diameter of the conduit.

Conduit density (*CD*), expressed as number of conduits per 1 mm^2 (Scholz et al. 2013), was calculated from the complete radial sectors considered for D_h calculations, dividing the total number of conduits by the sapwood area analyzed. The V_G is the ratio between total number of vessels and total number of vessel groupings (Carlquist 2001).

Pressure–volume analysis

Water potential isotherms (Tyree and Hammel 1972), also called pressure–volume (PV) curves, were measured in summer 2016 (i.e., during the third year of through-fall exclusion) in five samples (*F. sylvatica* leaves and *P. abies* end-twigs) per species and treatment. Curves were measured in July for *F. sylvatica* and in September for *P. abies* to ensure full maturation of tissues and completed xylogenesis in *P. abies* twigs.

Small branches were cut in late afternoon and rehydrated overnight, until water potential was >−0.2 MPa. Leaves of *F. sylvatica* or end-twigs of *P. abies* were detached with a razor blade, wrapped in cling film and initial water potential (Ψ_{leaf}/Ψ_{twig}) was measured with a pressure chamber (mod. 1505D, PMS Instrument co., Albany, OR, USA). Ψ_{leaf}/Ψ_{twig} and fresh mass were determined periodically during slow dehydration (cling film was removed) on the bench. Measurements stopped when the relation between water loss and Ψ_{leaf}^{-1} (or Ψ_{twig}^{-1}) became linear ($R^2 > 0.95$). The spreadsheet tool of Sack and Pasquet-Kok (2011) was used to determine the following PV traits: water potential at turgor loss point (Ψ_{TLP}, MPa; a key trait to assess plant species' ecological drought tolerance, Lenz et al. 2006, Bartlett et al. 2012), osmotic potential at full turgor (π_O, MPa) and bulk modulus of elasticity (ε, MPa, i.e., the slope of turgor potential versus relative water content, above and including turgor loss point).

Calculation of leaf/end-twig hydraulic conductance (K_{leaf} or K_{twig}, see below) required the determination of absolute leaf/end-twig capacitance, which is the ratio of changes in water content and respective Ψ_{leaf}/Ψ_{twig}, normalized by projected leaf area. Absolute leaf/end-twig capacitances were calculated at full turgor (i.e., above and including turgor loss point, C_{FT}, mmol m^{-2} MPa^{-1}) and below turgor loss point (C_{TLP}, mmol m^{-2} MPa^{-1}; see Brodribb and Holbrook 2003). Separate PV and capacitance analyses were made for entire control end-twigs (CO) and control segments grown in 2014 (CO_{year3}, see explanation above). As both methods are based on water potential measurements, cutting open a second end of twigs, as done for CO_{year3} end-twig segments, may cause the water column to relax and have an effect on the measured water potential. This effect was preliminarily checked to be very small and not significant.

Leaf/end-twig vulnerability

The response of hydraulic conductance (K_{leaf} in *F. sylvatica*, K_{twig} in spruce) to decreasing Ψ_{leaf}/Ψ_{twig} was measured in *F. sylvatica* leaves and *P. abies* end-twigs. K_{leaf}/K_{twig} were determined using the rehydration kinetics technique described by Brodribb and Holbrook (2003). Branches (of ~60 cm length) of seven to eight trees per treatment were harvested in the early morning, transported to the laboratory and wrapped in a plastic bag containing a wet paper towel, for at least 30 min, in order to equilibrate water potentials. Measurements were performed under laboratory conditions (air temperature of 20–23 °C and artificial light). Initial water potential (Ψ_O, MPa) was determined in two leaves (*F. sylvatica*) or end-twigs (*P. abies*): if the difference between the two Ψ_O was >0.1 MPa, measurements were discarded. A third leaf/end-twig was cut while the cut end immersed in filtered (0.2 µm), degassed, 10 mM KCl and 1 mM $CaCl_2$ solution and let rehydrate for a rehydration time (t) of 5–10 s for *F. sylvatica* and 30 to 70 s for *P. abies*. In *P. abies*, prior to excision, the region of the twig to be cut for rehydration was stripped of its bark to avoid resin occlusion at the cut surface. The rehydrated leaves/end-twigs were then wrapped in plastic cling for 2 min to allow for equilibration of water potential. Final water potential (Ψ_f, MPa) was measured and K_{leaf} (or K_{twig} in *P. abies*, mmol MPa^{-1} s^{-1} m^{-2}) was calculated as follows:

$$K_{leaf} = C_{FT}[ln(\Psi_O\Psi_f^{-1})]t^{-1} \quad (6)$$

When Ψ_O was below Ψ_{TLP}, C_{FT} was substituted by C_{TLP}. As for PV curves, separate vulnerability curves were made in control end-twig segments grown in 2014 (CO_{year3}).

Maximum leaf/end-twig conductance K_{max_leaf} (or K_{max_twig}) was calculated as mean K_{leaf} (or K_{twig}) of well hydrated shoots (Ψ_O >−0.8 MPa) and percentage loss of conductance calculated as PLC for stems (Eq. (1)), substituting k_i by $K_{max\_leaf}/K_{max\_twig}$ and k_f by K_{leaf}/K_{twig}. Leaf/end-twig vulnerability curves were plotted as sigmoidal functions following Eq. (2), where Ψ_{50_branch} was substituted by $\Psi_{50\_leaf}/\Psi_{50\_twig}$ (water potential inducing 50% loss of leaf/end-twig conductance) and a_{branch} by a_{leaf}/a_{twig}.

Leaf-to-stem safety margins

The leaf-to-stem safety margin was calculated as the difference between leaf/end-twig hydraulic safety (expressed as Ψ_{50_leaf} in *F. sylvatica* and as Ψ_{50_twig} in *P. abies*) and branch xylem hydraulic safety (expressed as Ψ_{50_branch}) for each treatment (i.e., $\Psi_{50\_leaf} - \Psi_{50\_branch}/\Psi_{50\_twig} - \Psi_{50\_branch}$).

Statistical analyses

Values are given as mean ± SE. For curve fitting, vulnerability data were pooled per treatment and segment (branches or leaves/end-twigs), while vulnerability thresholds were calculated per sample. All data were tested for normality (Shapiro–Wilk test) and homoscedasticity (Levene test). Branch vulnerability curve parameters (a_{branch}, Ψ_{12_branch}, Ψ_{50_branch} and Ψ_{88_branch}) were compared within and between species (four groups) with Welch *F*-test, followed by post hoc Games-Howell test. Student's *t*-test (when equal variances) or Welch *t*-test (when unequal variances) were used to test differences between CO and TE treatments in Ψ_{pd}, Ψ_{md}, anatomical parameters of both species and in PV traits, K_{max_leaf}, Ψ_{50_leaf} and a_{leaf} of *F. sylvatica*. In *P. abies*, PV traits, Ψ_{50_twig}, K_{max_twig} and a_{twig} were compared between CO, CO_{year3} and TE, using one-way ANOVA followed by Tukey-HSD post hoc test. All tests were performed at a probability level of $P < 0.05$ using SPSS (IBM SPSS Statistics for Windows, Version 23.0; IBM Corp., Armonk, NY, USA).

Results

Soil water content and pre-dawn water potentials

From the beginning of the through-fall exclusion (May 2014) on, SVWC was generally lower in precipitation-excluded (TE) than in control (CO) plots, in all the measured soil horizons (Figure 2; data not shown for 10–30 cm and 30–50 cm depths). The shallower horizons (0–7 and 10–30 cm), with respect to the deeper ones, showed the lowest SVWC and the highest differences between treatments. When the roofs were permanently open (over winter, see gray zones in Figure 2), water in the soil of TE plots was only partially recharged, due to scarce precipitation over winter 2014/15 as well as winter 2015/16. In summer 2015, CO plots reached similar low SVWC as TE plots because of a natural drought episode.

In both species and in all campaigns, pre-dawn water potentials (Ψ_{pd}) were lower in through-fall exclusion trees relative to CO (Table 1), supporting the effectiveness of the through-fall exclusion treatment and confirming SVWC data. Ψ_{pd} differences between treatments were ~0.2 MPa higher in *P. abies* than in *F. sylvatica*, with exception of August campaigns where scarce or absent precipitation events caused a drop of Ψ_{pd} in bot species at the CO plots (Table 1). The most pronounced differences were observed in *P. abies* in July 2015 with 0.8 MPa lower Ψ_{pd} in TE versus CO trees.

Branch xylem vulnerability to cavitation

Both species showed a more cavitation resistant xylem in TE than in CO trees and thus a shift in branch vulnerability upon experimental drought (Figure 3; Table 2). In *F. sylvatica*, Ψ_{50_branch} was 0.4 MPa lower in TE (−3.82 ± 0.05 MPa) than in CO trees (−3.42 ± 0.07 MPa) and Ψ_{12_branch} and Ψ_{88_branch} similarly shifted by ~0.5 and 0.3 MPa, respectively (Table 2). In *P. abies*, a similar trend was observed (although only significant regarding Ψ_{50_branch}), with an average of −3.74 ± 0.06 MPa in CO and of −4.09 ± 0.07 MPa in TE branches.

Overall, branches of *P. abies* exhibited slightly more negative vulnerability thresholds than *F. sylvatica* (CO trees; Table 2). The slope of the sigmoidal curves, indicated by the parameter a_{branch}, did not differ within and between species (Table 2).

Wood anatomical traits

The observed conduit mean arithmetic diameter (D), conduit mean hydraulic diameter (D_h) and conduit wall reinforcement $(t/b)_h^2$ in branch cross sections did not differ significantly between treatments in both species. However, *F. sylvatica* TE trees tended to have smaller vessels and higher conduit reinforcement, with D averaging ~15.1 and 12.3 μm ($P < 0.10$), D_h averaging ~28.2 and 27.4 μm and $(t/b)_h^2$ averaging ~1.4 and 1.8 in CO and TE, respectively (Table 3). In *F. sylvatica*, also conduit density (CD) was (significantly) higher in TE (1218 ± 74 mm^{-2}) with respect to CO branches (872 ± 113 mm^{-2}), while no difference was observed in *P. abies* (Table 3). The vessel grouping index (V_G) analyzed in *F. sylvatica* revealed no differences between treatments.

Pressure–volume traits

Both *F. sylvatica* and *P. abies* TE trees exhibited ~0.5 MPa lower leaf/end-twig water potentials at turgor loss point (Ψ_{TLP}) than CO trees. This adjustment in Ψ_{TLP} was based, in both species, on an ~0.4 MPa more negative osmotic potential at full turgor (π_O) in TE versus CO trees (Figure 4). In addition, a lower bulk modulus of elasticity (ε) was found in TE end-twigs of *P. abies*, indicating higher cell wall elasticity. In both species, absolute capacitances at full turgor (C_{FT}) and below turgor loss point (C_{TLP}, data not shown) did not significantly differ between treatments, even though they tended to be higher in TE than in CO leaves/twigs (Figure 4). Control end-twig segments grown in 2014 (CO_{year3}) of *P. abies*, showed intermediate Ψ_{TLP} and π_O, higher C_{FT} and C_{TLP}, and lower ε with respect to CO and TE twigs (Figure 4).

Total leaf/end-twig vulnerability, safety margins and minimum seasonal water potentials

Fagus sylvatica TE leaves lost 50% of hydraulic conductance at ~0.35 MPa more negative water potential (Ψ_{50_leaf}) than CO leaves. The average maximum whole-leaf hydraulic conductance (K_{max_leaf}) observed was 34.2 mmol MPa^{-1} s^{-1} m^{-2} in CO and 30.4 mmol MPa^{-1} s^{-1} m^{-2} in TE leaves (no significant difference; Table 2).

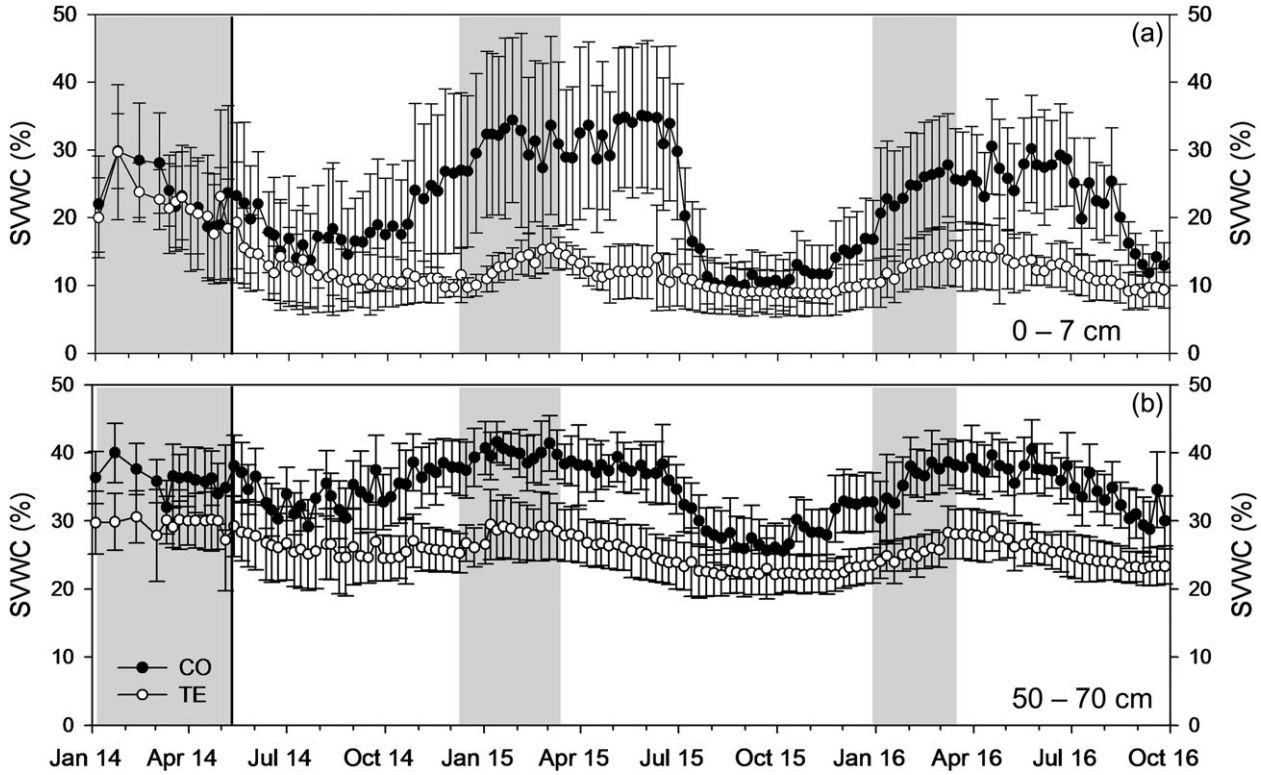

Figure 2. Soil volumetric water content (SVWC) at 0–7 cm (a) and 50–70 cm (b) depth. The SVWC was assessed weekly (January 2014 to September 2016) in CO and TE plots. The beginning of the through-fall exclusion (May 2014) is marked by a vertical black line. Gray background shows the time periods with permanently opened roofs (winter). Values are means ± SE ($n = 6$).

Table 1. Pre-dawn leaf water potentials (Ψ_{pd}, MPa) measured in five field campaigns within the three consecutive growing seasons subjected to through-fall exclusion (2014–16), in CO and TE treatments.

	Fagus sylvatica		*Picea abies*	
Date	CO	TE	CO	TE
18 July 2014	−0.42 ± 0.03	−0.75 ± 0.08**	−0.89 ± 0.06	−1.39 ± 0.05**
21 July 2015	−0.76 ± 0.05	−1.32 ± 0.05**	−0.79 ± 0.04	−1.60 ± 0.05**
14 August 2015	−1.31 ± 0.13	−1.66 ± 0.10*	−1.31 ± 0.09	−1.63 ± 0.11*
18 July 2016	−0.32 ± 0.01	−0.56 ± 0.03**	−0.52 ± 0.01	−1.03 ± 0.07**
25 August 2016	−0.38 ± 0.03	−0.78 ± 0.05**	−0.59 ± 0.03	−0.85 ± 0.11

Values are means ± SE ($n = 6$–8). *$0.01 < P < 0.05$; **$P < 0.01$ between treatments of a species.

In *P. abies*, mean Ψ_{50_twig} was 0.44 MPa lower in TE than in CO samples (Table 2). CO_{year3} samples showed intermediate Ψ_{50_twig} with respect to CO and TE end-twigs but the highest K_{max_twig} (42.1 ± 2.6 mmol MPa^{-1} s^{-1} m^{-2}). No difference in K_{max_twig} was found between CO and TE samples. In TE trees, leaf-to-stem safety margins of both species were overall similar to CO trees (Table 2).

Minimum Ψ_{md} measured in summer 2016 in *F. sylvatica* twigs was significantly lower in TE (−2.33 ± 0.10 MPa) than in CO trees (−1.97 ± 0.07 MPa; $P < 0.05$). In *P. abies*, no differences in minimum Ψ_{md} were found between CO (−1.95 ± 0.5 MPa) and TE (−2.09 ± 0.04 MPa) treatments.

Discussion

Acclimation of xylem hydraulic vulnerability

The through-fall exclusion experiment demonstrated that, under prolonged but overall moderate drought (see pre-dawn water potential data, Ψ_{pd}; Table 1), both study species exhibited significant and short-term acclimation in vulnerability to xylem cavitation (Figure 3). With respect to pre-dawn water potentials (Table 1), *P. abies* showed slightly higher levels of drought stress than *F. sylvatica* upon drought treatment. This can be explained by the shallow rooting system of *P. abies* (the majority of fine roots are restricted to the upper 30 cm; K.-H. Haeberle, personal

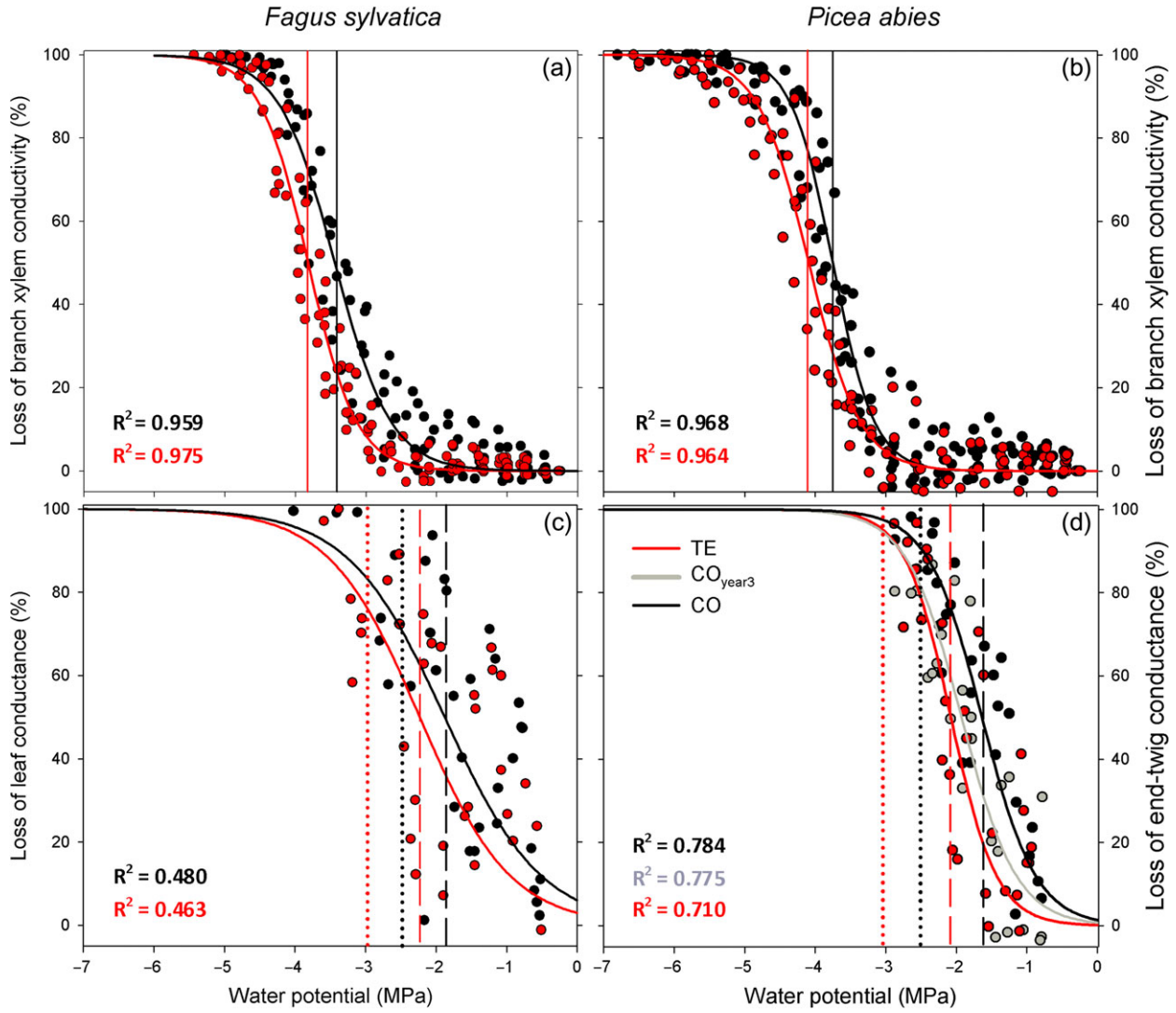

Figure 3. Branch (a, b) and terminal shoots (*F. sylvatica* leaves, c; *P. abies* end-twigs, d) vulnerability curves of CO and TE treatments. The vulnerability curve of *P. abies* control end-twig segments grown in 2014 (CO_{year3}) is shown in (d). Solid vertical lines indicate water potentials inducing 50% loss of branch xylem conductivity (Ψ_{50_branch}; $n = 7–8$), dotted vertical lines indicate water potentials at turgor loss point (Ψ_{TLP}) and dashed vertical lines indicate water potentials at 50% loss of leaf/twig conductance (Ψ_{50_leaf}/ Ψ_{50_twig}; $n = 7–8$).

communication) as upper soil layers developed the lowest water contents (Figure 2). During through-fall exclusion, in *P. abies* water uptake of TE trees almost stopped, while in *F. sylvatica* it continued, albeit at lower rates (C. Kallenbach, personal communication). Therefore, given that soil water content detected by sensors (reaching a maximum depth of 70 cm) did not further decrease during prolonged drought (Figure 2), it is very likely that *F. sylvatica* roots had access to water from deeper soil layers. Overall the difference in drought stress between species was minor and it is thus remarkable (and in contradiction to the hypothesis formulated in the Introduction) that not only the more anisohydric angiosperm *F. sylvatica* but also the isohydric conifer *P. abies* showed acclimation.

Previous studies showed plasticity in cavitation resistance of *F. sylvatica* (Herbette et al. 2010) and provided evidence of an environmental control of this hydraulic trait (Wortemann et al. 2011, Aranda et al. 2015). Accordingly, Schuldt et al. (2016) have recently shown an increase in cavitation resistance with decreasing water availability in *F. sylvatica* populations distributed along a geographical gradient of precipitation. Our results sustain and strengthen the above-cited findings. The applied through-fall exclusion system allowed the comparison of adult trees within the same forest stand and thus permitted us to exclude possible population genetic or site (e.g., nutrient availability and soil water storage capacity differences, Goldstein et al. 2013, Tokumoto et al. 2014) effects. *Picea abies* seedlings were found to become more vulnerable to xylem cavitation upon drought (Chmura et al. 2016), probably because of 'cavitation fatigue' (Hacke et al. 2001*b*). A dendrochronological study conducted in a mature *P. abies* plantation equipped with a through-fall exclusion system, instead, showed under drought the

Table 2. Branch and leaf/end-twig hydraulic vulnerability. Slope of branch xylem vulnerability curve (a_{branch}), water potential at 12 (Ψ_{12_branch}), 50 (Ψ_{50_branch}) and 88% (Ψ_{88_branch}) loss of branch xylem conductivity; slope of leaf/twig vulnerability curve (a_{leaf}/a_{twig}), water potential at 50% loss of leaf/end-twig conductance (Ψ_{50_leaf}/ Ψ_{50_twig}), maximum leaf/end-twig hydraulic conductance (K_{max_leaf}/ K_{max_twig}) and hydraulic safety margin ($\Psi_{50\_leaf} - \Psi_{50\_branch}$/ $\Psi_{50\_twig} - \Psi_{50\_branch}$).

	Fagus sylvatica		*Picea abies*		
	CO	TE	CO		TE
a_{branch}	2.73 ± 0.26^{a}	3.09 ± 0.18^{a}	3.72 ± 0.43^{a}		3.11 ± 0.35^{a}
Ψ_{12_branch} (MPa)	-2.64 ± 0.14^{a}	-3.16 ± 0.07^{b}	-3.15 ± 0.09^{b}		-3.39 ± 0.07^{b}
Ψ_{50_branch} (MPa)	-3.42 ± 0.07^{a}	-3.82 ± 0.05^{b}	-3.74 ± 0.06^{b}		-4.09 ± 0.07^{c}
Ψ_{88_branch} (MPa)	-4.19 ± 0.04^{a}	-4.48 ± 0.06^{b}	-4.33 ± 0.10^{ab}		-4.80 ± 0.16^{b}
	CO	TE	CO	CO_{year3}	TE
a_{leaf}/a_{twig}	1.46 ± 0.38^{a}	1.56 ± 0.42^{a}	2.62 ± 0.43^{a}	2.56 ± 0.45^{a}	3.08 ± 0.66^{a}
Ψ_{50_leaf}/ Ψ_{50_twig} (MPa)	-1.88 ± 0.16^{a}	-2.23 ± 0.17^{a}	-1.63 ± 0.07^{a}	-1.92 ± 0.07^{b}	-2.07 ± 0.08^{b}
K_{max_leaf}/ K_{max_twig} (mmol MPa^{-1} s^{-1} m^{-2})	34.2 ± 2.2^{a}	30.4 ± 3.2^{a}	33.1 ± 2.3^{a}	42.1 ± 2.6^{b}	35.4 ± 2.6^{a}
$\Psi_{50\_leaf} - \Psi_{50\_branch}$/ $\Psi_{50\_twig} - \Psi_{50\_branch}$ (MPa)	1.54	1.59	2.11	1.82	2.02

CO_{year3}, control end-twig segments grown in 2014. Different letters indicate significant differences ($P < 0.05$) across species and treatments for branch parameters, within species treatments for leaf/twig parameters. Values are means ± SE ($n = 7$–8).

Table 3. Conduit mean arithmetic diameter (D), conduit mean hydraulic diameter (D_h), conduit wall reinforcement [$(t/b)_h^2$], conduit density (CD) and vessel grouping index (V_G) calculated from cross sections of CO and TE branches ($n = 5$).

	Fagus sylvatica		*Picea abies*	
	CO	TE	CO	TE
D (μm)	15.1 ± 1.3*	12.3 ± 0.5*	9.8 ± 0.5	9.6 ± 0.3
D_h (μm)	28.2 ± 1.3	27.4 ± 1.3	13.9 ± 0.7	13.8 ± 0.4
$(t/b)_h^2 \times 10^{-2}$	1.44 ± 0.16	1.76 ± 0.27	7.26 ± 1.06	7.24 ± 1.00
CD (mm^{-2})	872 ± 113**	1218 ± 74**	3995 ± 192	3928 ± 153
V_G	2.51 ± 0.39	2.90 ± 0.27	–	–

*$0.05 < P < 0.1$; **$P < 0.05$ between treatments of a species. Values are means ± SE.

formation of conduits with smaller mean hydraulic diameter and higher cell wall reinforcement [$(t/b)_h^2$], which might be more resistant to cavitation (Montwé et al. 2014). In our study, a clear trend in anatomical parameters was overall lacking: just the increased wall reinforcement $(t/b)_h^2$ and CD (also see Giagli et al. 2016, Hajek et al. 2016, Schuldt et al. 2016) in TE branches of *F. sylvatica* might be related to increased cavitation resistance. It is likely that changes in pit architecture are more relevant for adjustments in hydraulic safety of both conifers (Hacke and Jansen 2009, Jansen et al. 2012, Bouche et al. 2014) and angiosperms (Lens et al. 2011), while anatomical parameters analyzed in the present study only partly or indirectly reflect functional hydraulic traits.

It should be noted that all branch samples of *F. sylvatica* were flushed to remove native embolism prior to vulnerability measurements. Due to potential cavitation fatigue (Hacke et al. 2001*b*), flushing might have caused a general overestimation of vulnerabilities but did not influence the observed differences between CO and TE branches as native embolism was similar (see 'Materials and methods' section). Moreover, requiring a sample length of 28 cm for the Cavitron technique, it was not possible to analyze branch segments entirely formed during the TE period. Accordingly, the central segment of these samples used for anatomical analysis, contained also xylem formed the year before the start of the drought treatment. Thus, it can be expected that xylem segments completely formed during the through-fall exclusion period would show even bigger shifts in Ψ_{50_branch} and in anatomical parameters than those observed. Despite this possible underestimation of drought effects, acclimation was proven to occur during only two growing seasons, in which drought was induced. Overall plasticity in cavitation resistance upon exposure to drought is probably species-specific. For instance, Martin-StPaul et al. (2013) did not find any acclimation in branch vulnerability in a 7-year precipitation exclusion experiment on *Quercus ilex*.

Acclimation in turgor loss point and leaf/end-twig vulnerability

Fagus sylvatica leaves showed significant acclimation in the water potential at the turgor loss point (Ψ_{TLP}; Figure 4), which enables TE trees to maintain turgescence of the foliage at lower water potentials. Corresponding trends in Ψ_{TLP} and osmotic potentials at full turgor (π_O) indicate adjustments in Ψ_{TLP} to be based on osmoregulation (e.g., Bartlett et al. 2012). The observed acclimation in Ψ_{TLP} thereby was similar to the acclimation in leaf hydraulic vulnerability ($\Psi_{50\_leaf}/\Psi_{50\_twig}$; vertical lines

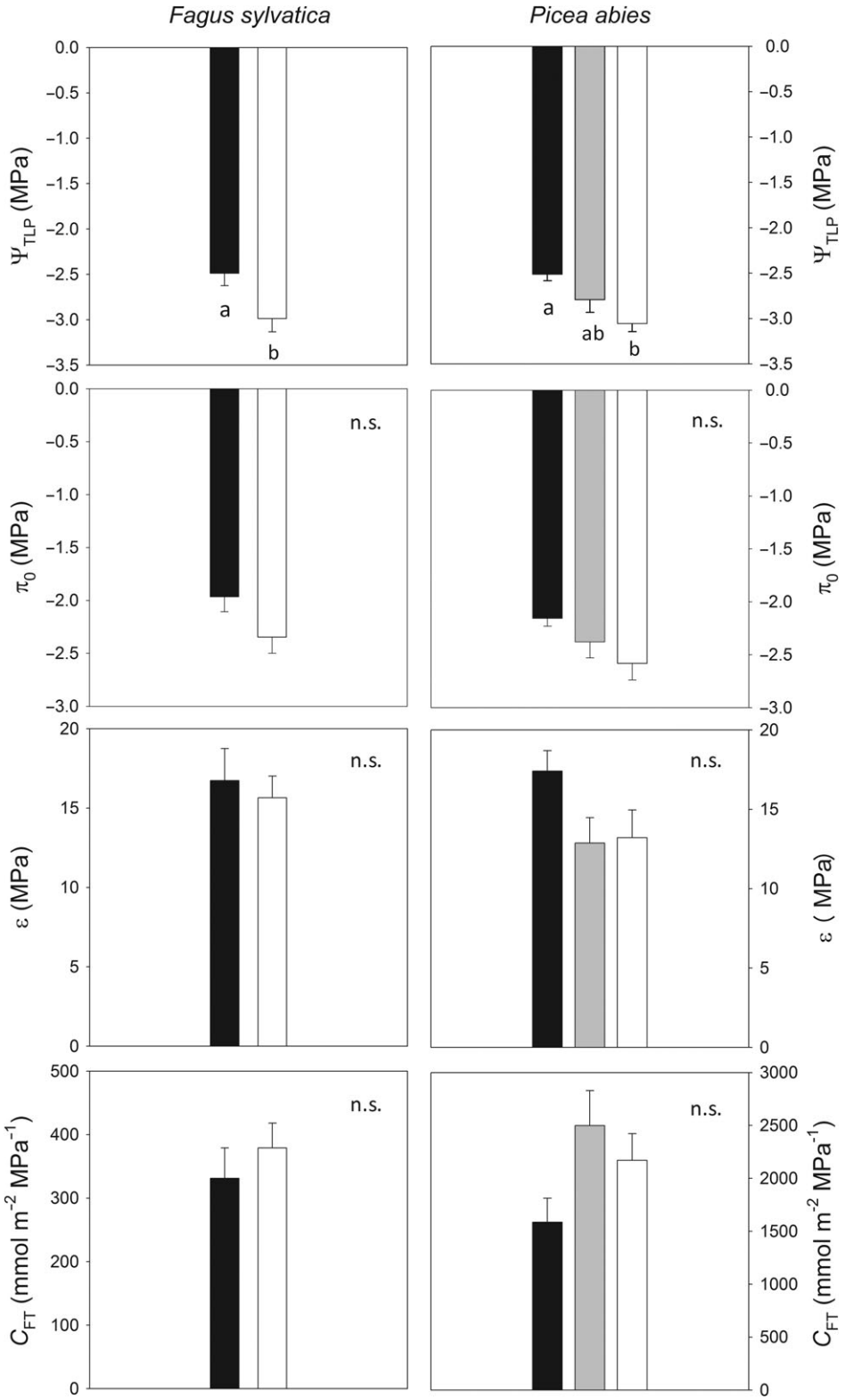

Figure 4. Leaf/end-twig pressure–volume parameters. In leaves (*F. sylvatica*) and end-twigs (*P. abies*) of CO (black bars), TE (white bars) and control segment (CO_{year3}, *P. abies*, gray bars) samples, were analyzed: water potential at turgor loss point (Ψ_{TLP}), osmotic potential at full turgor (π_O), bulk modulus of elasticity (ε) and absolute capacitance at full turgor (C_{FT}). Different letters indicate significant differences ($P < 0.05$) across treatments. Bars are means ± SE ($n = 6$ in *F. sylvatica*, $n = 5$ in *P. abies*).

Figure 3c), according to correlations between Ψ_{TLP} and leaf vulnerability published in previous studies (Blackman et al. 2010, Nardini and Luglio 2014, Martorell et al. 2015).

In *F. sylvatica* maximum leaf hydraulic conductance (K_{max_leaf}) was within the range reported for angiosperms (Brodribb et al. 2005), while K_{max_twig} of *P. abies* was much higher than the needle conductance reported for conifers (values between 1.6 and 24.1 mmol MPa^{-1} s^{-1} m^{-2}; Brodribb et al. 2005, Johnson et al. 2009, 2016, Charra-Vaskou and Mayr 2011). Differences in K_{max_twig} measurements are likely related to the definition of reference areas as K_{max_twig} calculations use a normalization by the projected leaf area (Brodribb and Holbrook 2003), not accounting for needle geometry. In *P. abies* needles, the total leaf area is 2.2–4.0 times the respective projected area (Sellin 2000).

The loss of hydraulic conductance in dehydrating leaves is the result of xylem cavitation (Nardini et al. 2001, Johnson et al. 2012*b*), partial leaf xylem collapse (e.g., Cochard et al. 2004) and reduction in the extra-xylary conductance (Heinen et al. 2009, Voicu et al. 2009, Scoffoni et al. 2014). All these mechanisms might be responsible for the observed adjustment in leaf vulnerability (Table 2; Figure 3), as in both species under study vulnerability thresholds of leaves/end-twigs were more negative in TE than in CO trees. However, in the case of *P. abies*, the observed difference may also be substantially based on the reduced growth of new flushes (Figure 1d) and less on acclimation. Accordingly, control end-twig segments grown in 2014 (CO_{year3}) and TE twigs (carrying very small shoots from the previous and current year) had similar Ψ_{50_twig}. In contrast, in intact CO sample twigs, the bigger proportion of younger twigs and needles (formed in the previous and current year) caused overall higher Ψ_{50_twig}. This also indicates age-related changes in the vulnerability of end-twigs, probably related to mesophyll developments and thus to extra-xylary pathways. Indeed, in the conifer *Pinus pinaster*, Charra-Vaskou et al. (2012) and Bouche et al. (2016) found the hydraulic safety of needle xylem to be similar to branch xylem and higher than in the entire needle, indicating extra-xylary components to be hydraulically limiting. Ontogenetic changes might also explain the shifts in Ψ_{TLP} and π_O observed in *P. abies* TE end-twigs, which are similar to the shifts in twig vulnerability (Figure 3d) as noted above for beech.

Coordination of hydraulics

Leaf-to-branch safety margins were positive and relatively wide in both species, whereby the safety margin was smaller in the more anisohydric *F. sylvatica* than in *P. abies* (Table 2).

According to the hydraulic segmentation hypothesis (Bucci et al. 2013, Pivovaroff et al. 2014), recently validated between branches and leaves of both angiosperm and conifer species (Johnson et al. 2016), our findings indicate that in both species leaves/needles act as hydraulic fuses, which protect proximal sections of hydraulic pathways. Considering the quantitatively similar and unidirectional changes in vulnerability of branches and leaves/end-twigs as well as in turgor upon drought, hydraulic traits and respective acclimations seem to be well coordinated within trees.

In *F. sylvatica* minimum water potentials (Ψ_{md}) measured in the field in summer 2016 were in both treatments similar to Ψ_{50_leaf} calculated from vulnerability curves (Table 2). This indicates that stomata regulate in dependence of the hydraulic limits (and thus vulnerabilities) of the distal components of the hydraulic pathway. In contrast, TE end-twigs of *P. abies* had a lower risk of hydraulic dysfunction due to their higher leaf hydraulic resistance and the absence of changes in Ψ_{md}. Reductions in conductivity located in extra-xylary part of leaves/twigs might be reversible (Cochard et al. 2004, Scoffoni et al. 2014) so that the observed Ψ_{md} were still safe for the hydraulic integrity of leaves/twigs.

Conclusion

Despite obvious contrasts in xylem anatomy, foliage type, crown architecture and ecophysiology (including hydraulic strategies), the co-occurring *F. sylvatica* and *P. abies* showed analogous hydraulic adjustments, well coordinated between branch and leaf/end-twig levels. In *P. abies*, growth limitation (production of very small twigs) might indicate a possible trade-off between increased hydraulic safety and decreased productivity. The results of the through-fall exclusion experiment thus suggest that the forest species studied might exhibit sufficient hydraulic plasticity to better cope with future drought periods. As hydraulic acclimation was observed upon relatively mild but prolonged drought, our experiment also highlights the importance of long-term field drought experiments. More intense or longer droughts, however, may exceed the species' capacity for hydraulic acclimation (Gutschick and BassiriRad 2003), and mild but extremely prolonged droughts may in the long term induce consumption of carbohydrate reserves to critical levels (McDowell et al. 2008). Moreover, trees weakened by hydraulic limitation and/or carbon-starvation are usually also more susceptible to biotic attacks (Schlyter et al. 2006). All these variables might affect tree species differently and modify competition between co-occurring species. Further field studies in natural or managed eco-systems are urgently needed to estimate the performance of tree species under future climate.

Supplementary Data

Supplementary Data for this article are available at *Tree Physiology* Online.

Acknowledgments

We acknowledge the technical assistance of Thomas Feuerbach, Josef Heckmair and Peter Kuba within the KROOF experiment and Dr Michael Goisser for field sampling help.

Conflict of interest

None declared.

Funding

M.T. acknowledges the support of the TUM 'International Graduate School of Science and Engineering' (IGSSE) through the Deutsche Forschungsgemeinschaft (DFG). The KROOF experiment is funded by the Bavarian State Ministries of the Environment and Consumer Protection, and of Food, Agriculture and Forestry and by the DFG. Parts of the study were supported by a Sparkling Science Project funded by the Federal Ministry of Science, Research and Economy (Bundesministerium fuer Wissenschaft, Forschung und Wirtschaft), Austria and a Hertha-Firnberg Project (T667-B16 'Hydraulics of juvenile trees') funded by the Austrian Science Fund (FWF).

References

Allen CD, Macalady AK, Chenchouni H et al. (2010) A global overview of drought and heat-induced tree mortality reveals emerging climate change risks for forests. For Ecol Manage 259:660–684.

Ambrose AR, Sillett SC, Dawson TE (2009) Effects of tree height on branch hydraulics, leaf structure and gas exchange in California redwoods. Plant Cell Environ 32:743–757.

Anderegg WRL (2015) Spatial and temporal variation in plant hydraulic traits and their relevance for climate change impacts on vegetation. New Phytol 205:1008–1014.

Aranda I, Cano FJ, Gascó A, Cochard H, Nardini A, Mancha JA, Lopez R, Sanchez-Gomez D (2015) Variation in photosynthetic performance and hydraulic architecture across European beech (*Fagus sylvatica* L.) populations supports the case for local adaptation to water stress. Tree Physiol 35:34–46.

Bartlett MK, Scoffoni C, Sack L (2012) The determinant of leaf turgor loss point and prediction of drought tolerance of species and biomes: a global meta-analysis. Ecol Lett 15:393–405.

Beikircher B, Mayr S (2009) Intraspecific differences in drought tolerance and acclimation in hydraulics of *Ligustrum vulgare* and *Viburnum lantana*. Tree Physiol 29:765–775.

Beikircher B, Mayr S (2016) Avoidance of harvesting and sampling artefacts in hydraulic analyses: a protocol tested on *Malus domestica*. Tree Physiol 36:797–803.

Beikircher B, Ameglio T, Cochard H, Mayr S (2010) Limitation of the cavitron technique by conifer pit aspiration. J Exp Bot 61:3385–3393.

Beikircher B, De Cesare C, Mayr S (2013) Hydraulics of high-yield orchard trees: a case study of three *Malus domestica* cultivars. Tree Physiol 33:1296–1307.

Blackman CJ, Brodribb TJ, Jordan GJ (2010) Leaf hydraulic vulnerability is related to conduit dimensions and drought resistance across a diverse range of woody angiosperms. New Phytol 188:1113–1123.

Bouche PS, Larter M, Domec JC, Burlett R, Gasson P, Jansen S, Delzon S (2014) A broad survey of hydraulic and mechanical safety in the xylem of conifers. J Exp Bot 65:4419–4431.

Bouche PS, Delzon S, Choat B et al. (2016) Are needles of *Pinus pinaster* more vulnerable to xylem embolism than branches? New insights from X-ray computed tomography. Plant Cell Environ 39:860–870.

Briffa KR, van der Schrier G, Jones PD (2009) Wet and dry summers in Europe since 1750: evidence of increasing drought. Int J Climatol 29: 1894–1905.

Brodribb TJ, Holbrook NM (2003) Stomatal closure during leaf dehydration, correlation with other leaf physiological traits. Plant Physiol 132: 2166–2173.

Brodribb TJ, Holbrook NM, Zwieniecki MA, Palma B (2005) Leaf hydraulic capacity in ferns, conifers and angiosperms: impacts on photosynthetic maxima. New Phytol 165:839–846.

Bucci SJ, Scholz FG, Peschiutta ML, Arias NS, Meinzer FC, Goldstein G (2013) The stem xylem of Patagonian shrubs operates far from the point of catastrophic dysfunction and is additionally protected from drought-induced embolism by leaves and roots. Plant Cell Environ 36: 2163–2174.

Carlquist S (2001) Comparative wood anatomy—systematic, ecological, and evolutionary aspects of Dycotiledon wood, 2nd edn. Springer, Berlin.

Charra-Vaskou K, Mayr S (2011) The hydraulic conductivity of the xylem in conifer needles (*Picea abies* and *Pinus mugo*). J Exp Bot 62: 4383–4390.

Charra-Vaskou K, Badel E, Burlett R, Cochard H, Delzon S, Mayr S (2012) Hydraulic efficiency and safety of vascular and non-vascular components in *Pinus pinaster* leaves. Tree Physiol 32:1161–1170.

Chmura DJ, Guzicka M, McCulloh KA, Zytkowiak R (2016) Limited variation found among Norway spruce half-sib families in physiological response to drought and resistance to embolism. Tree Physiol 36: 252–266.

Cochard H (2002) A technique for measuring xylem hydraulic conductance under high negative pressures. Plant Cell Environ 25:815–819.

Cochard H, Froux F, Mayr S, Coutand C (2004) Xylem wall collapse in water-stressed pine needles. Plant Physiol 134:401–408.

Cochard H, Damour G, Bodet C, Tharwat I, Poirier M, Ameglio T (2005) Evaluation of a new centrifuge technique for rapid generation of xylem vulnerability curves. Physiol Plant 124:410–418.

Cornwell WK, Bhaskar R, Sack L, Cordell S, Lunch CK (2007) Adjustment of structure and function of Hawaiian *Metrosideros polymorpha* at high vs. low precipitation. Funct Ecol 21:1063–1071.

Dai A (2013) Increasing drought under global warming in observations and models. Nat Clim Chang 3:52–58.

Debat V, David P (2001) Mapping phenotypes: canalization, plasticity and developmental stability. Trends Ecol Evol 16:555–561.

Fuhrer J, Beniston M, Fischlin A, Frei C, Goyette S, Jasper K, Pfister C (2006) Climate risks and their impact on agriculture and forests in Switzerland. Clim Change 79:79–102.

Giagli K, Gricar J, Vavrcik H, Mensik L, Gryc V (2016) The effects of drought on wood formation in *Fagus sylvatica* during two contrasting years. IAWA J 37:332–348.

Goisser M, Geppert U, Roetzer T et al. (2016) Does belowground interaction with *Fagus sylvatica* increase drought susceptibility of photosynthesis and stem growth in *Picea abies*? For Ecol Manage 375: 268–278.

Goldstein G, Bucci SJ, Scholz FG (2013) Why do trees adjust water relations and hydraulic architecture in response to nutrient availability? Tree Physiol 33:238–240.

Gutschick VP, BassiriRad H (2003) Extreme events as shaping physiology, ecology and evolution of plants: toward a unified definition and evaluation of their consequences. New Phytol 160:21–42.

Hacke UG, Jansen S (2009) Embolism resistance of three boreal conifer species varies with pit structure. New Phytol 182:675–686.

Hacke UG, Sperry JS, Pockmann WT, Davis SD, McCulloh KA (2001*a*) Trends in wood density and structure are linked to prevention of xylem implosion by negative pressure. Oecologia 126:457–461.

Hacke UG, Stiller V, Sperry JS, Pittermann J, McCulloh KA (2001*b*) Cavitation fatigue: Embolism and refilling cycles can weaken the cavitation resistance of xylem. Plant Physiol 125:779–786.

Hajek P, Kurjak D, von Wuehlisch G, Delzon S, Schuldt B (2016) Intraspecific variation in wood anatomical, hydraulic, and foliar traits in

ten European beech provenances differing in growth yield. Front Plant Sci 7:791.
Heinen RB, Ye Q, Chaumont FO (2009) Role of aquaporins in leaf physiology. J Exp Bot 60:2971–2985.
Hera U, Roetzer T, Zimmermann L, Schulz C, Maier H, Weber H, Koelling C (2011) Klima en dètail-Neue hochaufgelöste Klimakarten zur klimatischen Regionalisierung Bayerns. LWF aktuell 19:34–37.
Herbette S, Wortemann R, Awad H, Huc R, Cochard H, Barigah TS (2010) Insights into xylem vulnerability to cavitation in *Fagus sylvatica* L.: phenotypic plasticity and environmental sources of variability. Tree Physiol 30:1448–1455.
Jacobsen AL, Pratt RB, Davis SD, Ewers FW (2007) Cavitation resistance and seasonal hydraulics differ among three arid Californian plant communities. Plant Cell Environ 30:1599–1609.
Jansen S, Lamy JB, Burlett R, Cochard H, Gasson P, Delzon S (2012) Plasmodesmatal pores in the torus of bordered pit membranes affect cavitation resistance of conifer xylem. Plant Cell Environ 35:1109–1120.
Johnson DM, Meinzer FC, Woodruff DR, McCulloh KA (2009) Leaf xylem embolism, detected acoustically and by cryo-SEM, corresponds to decreases in leaf hydraulic conductance in four evergreen species. Plant Cell Environ 32:828–836.
Johnson DM, McCulloh KA, Meinzer FC, Woodruff DR, Eissenstat DM (2011) Hydraulic patterns and safety margins, from stem to stomata, in three eastern US tree species. Tree Physiol 31:659–668.
Johnson DM, McCulloh KA, Woodruff DR, Meinzer FC (2012*a*) Hydraulic safety margins and embolism reversal in stems and leaves: why are conifers and angiosperms so different? Plant Sci 195:48–53.
Johnson DM, McCulloh KA, Woodruff DR, Meinzer FC (2012*b*) Evidence for xylem embolism as primary factor in dehydration-induced declines in leaf hydraulic conductance. Plant Cell Environ 35:760–769.
Johnson DM, Wortemann R, McCulloh KA, Jordan-Meille L, Ward E, Warren JM, Palmroth S, Domec JC (2016) A test of the hydraulic vulnerability segmentation hypothesis in angiosperm and conifer tree species. Tree Physiol 36:983–993.
Lamy JB, Delzon S, Bouche PS, Alia R, Vendramin GG, Cochard H, Plomion C (2014) Limited genetic variability and phenotypic plasticity detected for cavitation resistance in a Mediterranean pine. New Phytol 201:874–886.
Lemoine D, Jacquemin S, Granier A (2002) Beech (*Fagus sylvatica* L.) branches show acclimation of xylem anatomy and hydraulic properties to increased light after thinning. Ann For Sci 59:761–766.
Lens F, Sperry JS, Christman MJ, Choat B, Rabaey D, Jansen S (2011) Testing hypothesis that link wood anatomy to cavitation resistance and hydraulic conductivity in the genus *Acer*. New Phytol 190:709–723.
Lenz TI, Wright IJ, Westboy M (2006) Interrelations among pressure-volume curve traits across species and water availability gradients. Physiol Plant 127:423–433.
Lyr H, Fiedler HJ, Tranquillini W (1992) Physiologie und Ökologie der Gehölze. G. Fisher, Jena.
Maherali H, Pockman WT, Jackson RB (2004) Adaptive variation in the vulnerability of woody plants to xylem cavitation. Ecology 85:2184–2199.
Martinez-Vilalta J, Cochard H, Mencuccini M et al. (2009) Hydraulic adjustment of Scots pine across Europe. New Phytol 184:353–364.
Martin-StPaul N, Limousin JM, Vogt-Schilb H, Rodríguez-Calcerrada J, Rambal S, Longepierre D, Misson L (2013) The temporal response to drought in a Mediterranean evergreen tree: comparing a regional precipitation gradient and a throughfall exclusion experiment. Glob Chang Biol 19:2413–2426.
Martorell S, Medrano H, Tomàs M, Escalona JM, Flexas J, Diaz-Espejo A (2015) Plasticity of vulnerability to leaf hydraulic dysfunction during acclimation to drought in grapevines: an osmotic-mediated process. Physiol Plant 153:381–391.
McDowell N, Pockman WT, Allen CD (2008) Mechanisms of plant survival and mortality during drought: why do some plants survive while others succumb to drought? New Phytol 178:719–739.
Montwé D, Spiecker H, Hamann A (2014) An experimentally controlled extreme drought in a Norway spruce forest reveals fast hydraulic response and subsequent recovery of growth rates. Trees 28:891–900.
Nardini A, Luglio J (2014) Leaf hydraulic capacity and drought vulnerability: possible trade-offs and correlations with climate across three major biomes. Funct Ecol 28:810–818.
Nardini A, Tyree M, Salleo S (2001) Xylem cavitation in the leaf of *Prunus laurocerasus* and its impact on leaf hydraulics. Plant Physiol 125:1700–1709.
Nardini A, Battistuzzo M, Savi T (2013) Shoot desiccation and hydraulic failure in temperate woody angiosperms during an extreme summer drought. New Phytol 200:322–329.
Nolf M, Creek D, Duursma R, Holtum J, Mayr S, Choat B (2015) Stem and leaf hydraulic properties are finely coordinated in three tropical rain forest tree species. Plant Cell Environ 38:2652–2661.
Pammenter NW, Vander Willingen C (1998) A mathematical and statistical analysis of the curves illustrating vulnerability of xylem cavitation. Tree Physiol 18:589–593.
Pivovaroff AL, Sack L, Santiago LS (2014) Coordination of stem and leaf hydraulic conductance in southern California shrubs: a test of the hydraulics segmentation hypothesis. New Phytol 203:842–850.
Pretzsch H, Roetzer T, Matyssek R, Grams TEE, Haeberle KH, Pritsch K, Kerner R, Munch JC (2014) Mixed Norway spruce (*Picea abies* (L.) Karst) and European beech (*Fagus sylvatica* (L.)) stands under drought: from reaction pattern to mechanism. Trees 28:1305–1321.
Pretzsch H, Bauerle T, Haeberle KH, Matyssek R, Schuetze G, Roetzer T (2016) Tree diameter growth after root trenching in a mature mixed stand of Norway spruce (*Picea abies* (L.) Karst) and European beech (*Fagus sylvatica* (L.)). Trees 30:1761–1773.
Rita A, Cherubini P, Leonardi S, Todaro L, Borghetti M (2015) Functional adjustments of xylem anatomy to climatic variability: insights from long-term *Ilex aquifolium* tree-rings series. Tree Physiol 35:817–828.
Sack L, Pasquet-Kok J (2011) Leaf pressure-volume curve parameters. http://prometheuswiki.publish.csiro.au/tikicitation.php?page=Leaf%20pressurevolume%20curve%20parameters#sthash.1KxZH2vQ.dpuf (31 October 2017, date last accessed)
Schlyter P, Stjernquist I, Bärring L, Joensson AM, Nilsson C (2006) Assessment of the impacts of climate change and weather extremes on boreal forests in northern Europe, focusing on Norway spruce. Clim Res 31:75–84.
Scholz A, Klepsch M, Karimi Z, Jansen S (2013) How to quantify conduits in wood? Front Plant Sci 4:53.
Scholz FG, Bucci SJ, Goldstein G (2014) Strong hydraulic segmentation and leaf senescence due to dehydration may trigger die-back in *Nothofagus dombeyi* under severe droughts: a comparison with the co-occurring *Austrocedrus chilensis*. Trees 28:1475–1487.
Schuldt B, Knutzen F, Delzon S, Jansen S, Mueller-Haubold H, Burlett R, Clough Y, Leuschner C (2016) How adaptable is the hydraulic system of European beech in the face of climate change-related precipitation reduction? New Phytol 210:443–458.
Scoffoni C, Vuong C, Diep S, Cochard H, Sack L (2014) Leaf shrinkage with dehydration: coordination with hydraulic vulnerability and drought tolerance. Plant Physiol 164:1772–1788.
Sellin A (2000) Estimating the needle area from geometric measurements: application of different calculation methods to Norway spruce. Trees 14:215–222.
Sperry JS, Hacke UG (2004) Analysis of circular bordered pit function. I Angiosperm vessels with homogeneous pit membranes. Am J Bot 91: 369–385.
Soudzilovskaia NA, Elumeeva TG, Onipchenko VG, Shidakov II, Salpagarova FS, Khubiev AB, Tekeev DK, Cornelissen JH (2013) Functional traits predict relationships between plant abundance dynamic and long-term climate warming. Proc Natl Acad Sci USA 110:18180–18184.
Sultan SE (2000) Phenotypic plasticity for plant development, function and life history. Trends Plant Sci 5:537–542.

Taiz L, Zeiger E (2010) Plant physiology, 5th edn. Sinauer Associates Inc, Sunderland, MA.

Tokumoto I, Heilman JL, Schwinning S, McInnes KJ, Litvak ME, Morgan CLS, Kamps RH (2014) Small-scale variability in water storage and plant available water in shallow, rocky soils. Plant Soil 385:193–204.

Tyree MT, Ewers FW (1991) The hydraulic architecture of trees and other woody plants. New Phytol 119:345–360.

Tyree MT, Hammel HT (1972) The measurement of the turgor pressure and the water relations of plants by the pressure-bomb technique. J Exp Bot 23:267–282.

Tyree MT, Zimmermann MH (2002) Xylem structure and the ascent of sap, 2nd edn. Spriger, Berlin.

Voicu MC, Cooke JEK, Zwiazek JJ (2009) Aquaporin gene expression and apoplastic water flow in bur oak (*Quercus macrocarpa*) leaves in relation to the light response of leaf hydraulic conductance. J Exp Bot 60:4063–4075.

Wortemann R, Herbette S, Barigah TS, Fumanal B, Alia R, Ducousso A, Gomory D, Roeckel-Drevet P, Cochard H (2011) Genotypic variability and phenotypic plasticity of cavitation resistance in *Fagus sylvatica* L. across Europe. Tree Physiol 31:1175–1182.